lubricants

MDPI

Article

Experimental Study on Flexible Fiber Assisted Shear Thickening Polishing for Cutting Edge Preparation of Core Drill

Lanying Shao [1,2], Yu Zhou [1,2], Yanfei Dai [1,2] and Binghai Lyu [1,2,*]

[1] College of Mechanical Engineering, Zhejiang University of Technology, Hangzhou 310023, China
[2] Key Laboratory of Special Purpose Equipment and Advanced Processing Technology, Ministry of Education and Zhejiang Province, Zhejiang University of Technology, Hangzhou 310014, China
* Correspondence: icewater7812@126.com

Abstract: To improve the cutting performance of the core drill, the flexible fiber assisted shear-thickening polishing (FF-STP) for cutting edge preparation was proposed to eliminate the microscopic defect and obtain proper radius of the cutting edge of the core drill. The flexible fiber was introduced into the shear-thickening polishing process to break the thickened agglomerates and improve the efficiency of cutting edge preparation. The influence of the polishing speed, abrasive concentration and the flexible fiber contact length with the core drill on the cutting edge radius *r* and surface morphology of the core drill edge was analyzed, and the drilling experiments were carried out after preparation, the cutting heat and drilled holes' roughness were employed as evaluation indexes to evaluate the performance of the core drill. The results show that the cutting edge radius increases with the increase of polishing speed, abrasive concentration and contact length. However, too high a polishing speed and contact length reduce the abrasive particles involved in the polishing process, and then lead to a decline in preparation efficiency. Under the selected processing conditions, the cutting edge radius increases from the initial 5 μm to 14 μm and 27 μm with 4 min of treatment and 6 min of treatment preparation, respectively. The sharp cutting edge becomes rounded, the burrs and chipping on the cutting edge are eliminated, and the average roughness (R_a) of the flank face decreases from 110.4 ± 10 nm to 8.0 ± 3 nm. Nine holes were drilled consecutively by core drills after cutting edge preparation, and the cutting temperature and drilled holes' roughness were recorded. The maximum cutting temperature (122.4 °C) in the process with the prepared core drill (radius r = 14 μm) is about 20 °C lower than that with untreated one, and the roughness of the drilled hole (R_a 510.5 nm) about 189.9 nm lower. The results indicates that FF-STP is a promising method for high consistency preparation of the core drill cutting edge.

Keywords: core drill; shear-thickening polishing; flexible fiber; cutting edge preparation; edge radius; cutting temperature; roughness

Citation: Shao, L.; Zhou, Y.; Dai, Y.; Lyu, B. Experimental Study on Flexible Fiber Assisted Shear Thickening Polishing for Cutting Edge Preparation of Core Drill. *Lubricants* **2023**, *11*, 58. https://doi.org/10.3390/lubricants11020058

Received: 12 January 2023
Revised: 27 January 2023
Accepted: 30 January 2023
Published: 31 January 2023

1. Introduction

Machine parts with holes are an indispensable part in the engineering field. There are many ways to manufacture holes, which can be divided into grinding, reaming, broaching, boring, drilling, countersinking and so on [1]. The surface roughness, burrs, hole size and circularity determine the hole quality [2]. Drilling is a commonly used hole processing method. Its operation is simple but the process is complex. The performance of the tool greatly affects the quality of the drilling.

The core drill, also known as steel plate drill, adopts a multi-blade annular cutting configuration, and is mainly for the processing of steel material components. The drilling efficiency of core drill is 8–10 times that of the traditional twist drill [3]. A carbide steel core drill is made of high-strength alloy steel body and carbide inserts by welding [3]. Cemented carbide materials have high hardness and wear resistance. In developed countries, more than 90% of turning tools and more than 55% of milling tools are made of cemented

carbide [4]. However, there are still problems of the cemented carbide tools such as rapid wear of the drill edge and difficulty in guaranteeing the drilling quality during the processing. In order to improve the cutting performance and service life of the core drill, it is particularly important to well prepare the edge of the core drill after grinding.

Cutting edge preparation is an important process that determines the quality of the edge of the tool, and the cost of cutting edge preparation accounts for 24–34% of the total cost of tool manufacturing [5]. Tool life and performance depend decisively on the geometry of the cutting edge. A properly shaped cutting edge increases tool wear resistance, life and process reliability. There are defects on the surface of the cutting edge after grinding such as burrs, notches, and surface roughness. These defects can be effectively eliminated by reasonable cutting edge preparation, and the performance and service life of the tool can be improved. At present, there are many kinds of preparation methods, including drag finishing, electrochemical machining, laser machining and so on for cemented carbide tools. Li et al. [6] used abrasive electrolytic machining to prepare cemented carbide cutting tools, which can accurately process arc-shaped cutting edges, eliminate small edge chipping defects and nearby front/rear edge grinding marks, and the surface roughness reduced from 0.31 μm to 0.14 μm. Biermann et al. [7] used the sandblasting method to prepare the cemented carbide drill bit, and found that selectively changing the microstructure of the cutting edge can effectively improve the surface quality of the tool and prolong the service life. Zou [8] conducted a preparation test on a flat end mill through a new ultrasonic vibration cutting edge preparation machine. It was found that the preparation efficiency with the assistance of ultrasonic vibration was better than that of the preparation method without vibration, and the cutting edge radius was prepared to 18 μm, and the ultrasonic vibration method could be about 8 min faster, and the efficiency was increased by about 26%; Lv et al. [9] used four different abrasive media to drag the cutting edge preparation experiment of the solid carbide end milling cutter, and compared the cutting edge preparation effect of the four abrasive media from the aspects of material removal rate, edge shape and surface morphology. After 20 min of processing under the optimal abrasive medium, the edge radius increases from 3 μm to 15 μm. Peter et al. [10] carried out cutting edge preparation experiments on cemented carbide milling cutters and found that the rounded radius of the cutting edge was mainly affected by the spindle speed, which increased with the increase of spindle speed. After preparation, the difference between the rounded radius of cutting edge measured on the rake face and the helical face (flank face) is up to 15~16 μm. Bergs et al. [11] used a high temperature resistant diamond abrasive brush to carry out cutting edge preparation experiments on rotary cutting tools such as cemented carbide drills. The experimental results show that various symmetrical and asymmetrical edges can be obtained by changing process parameters such as cutting speed, feed rate and transverse feed depth. Kang et al. [12] conducted a cutting edge preparation test on a hard blade using a picosecond laser radiation method. It was found that under the conditions of wavelengths of 1064 nm (IR) and 532 nm (VIS) and 70 % spatial pulse overlap, the optimal surface quality below Ra 0.15 μm and the cutting edge with a clear profile of 20~40 μm radius can be obtained. Tomáš et al. [13] prepared cemented carbide turning blade edges by plasma discharge in electrolyte, which used plasma film to control the current during preparation. The radius of the blade increased from 10 μm to 45 μm after 50 s processing. Yussefian et al. [14] used foil paper as the counterface in EDM to perform cutting edge preparation experiments on cemented carbide inserts. Since the shape and size of the cutting edge after processing are only related to the thickness of foil paper, the uniformity of the cutting edge radius after preparation is significantly improved. Liu et al. [15] used micro-blasting jet technology to effectively prepare the cutting edge of the carbide insert YT15, eliminate microscopic defects and reduce the roughness of the edge, improve edge quality. Although the above methods can play a good role in preparation of tool cutting edges, there are problems such as preparation consistency and low efficiency. Therefore, it is necessary to explore a new type of tool cutting edge preparation method.

The shear-thickening polishing (STP) method is a newly developed polishing method that uses the rheological properties of non-Newtonian fluids under shear stress to achieve surface polishing. It has good adaptability to complex curved surfaces and can achieve high-efficiency and high-quality polishing [16–18]. Yang et al. [19] used the chemically enhanced force-rheological method to polish the aluminum alloy cone mirror for 20 min, and the surface roughness (R_a) was reduced from 64.9 nm to 8.1 nm, in such a way that the surface defects on cutting were almost eliminated. Lyu et al. [20] employed the shear-thickening polishing (STP) method to achieve effective polishing of the cemented carbide insert with complex shape. Although the surface roughness of the tip cutting edge reaches a low value (R_a 7.1 nm), the surface roughness of the root cutting edge remains a relatively high value (R_a 63.9 nm). Shao et al. [21] performed shear rheological polishing on quartz glass. After 8 minute's polishing, the surface roughness R_a decreased from (110 ± 10) nm to (1.2 ± 0.3) nm, and the MRR reached 165.2 nm/min. Lyu et al. [22] presented a novel method for polishing using brush tool-assisted shear-thickening polishing (B-STP), the average surface roughness R_a of the seven measuring points on the cutting edge decreased from 118.01 to 8.13 nm in 10 min polishing, while the standard deviation decreased from 7.40 to only 0.3 nm. Chan [23] et al. showed that asymmetric and symmetrical cutting edges can be produced by honing tool edges using non-Newtonian fluids. Span [24] et al. presented a proof-of-concept of an innovative finish machining process wherein material is removed by abrasives suspended in a dense aqueous mixture of cornstarch; the efficacy of this process for honing the edge of a cutting tool was investigated, the edge radius changed from initial 5 μm to 39 μm in 5 min. Shao [25] et al. conducted experiments on flexible fiber-assisted shear-thickening polishing for cemented carbide insert cutting edge preparation. The experimental results showed that the cutting edge preparation efficiency is the highest under the polishing angle of 10°, where the cutting edge radius increased from 15 ± 2 μm to 110 ± 5 μm in 5 min and the cutting edge shape can be controlled by adjusting the polishing angle, and K-factor varies from 0.14 ± 0.03 to 0.56 ± 0.05.

In this paper, the flexible fiber-assisted shear-thickening polishing (FF-STP) method is carried out to prepare the cutting edge of the core drill with cemented carbide material. The effects of polishing speed, abrasive concentration and the flexible fiber contact length with the core drill on the cutting edge radius and surface morphology of the core drill edge were discussed, and the drilling experiments were carried out to test whether the performance of the core drill was improved after cutting edge preparation.

2. The FF-FRP Principle

The FF-FRP principle of the core drill is shown in Figure 1. The polishing slurry is made from non-Newtonian fluid; the abrasive particles are uniformly dispersed in the non-Newtonian fluid. During the polishing process, the polishing slurry rotates with the polishing tank and moves relative to the core drill installed on the fixture, the shear-thickening effect occurs in the contact area between the workpiece and the polishing slurry under the applied shear stress when the relative velocity exceeds a threshold, and the solid colloidal particles dispersed in the polishing slurry are aggregated. In the contact area, a large number of particle clusters wrapped in abrasive particles are formed, meanwhile, with the viscosity of polishing slurry rising sharply, the slurry shows a quasi-solid state, which enhances the holding force of the abrasive particles and forms a "flexible fixed abrasive tool" at the processing position, then, the core drill edge will be prepared through the micro-cutting action of abrasive particles. However, the polishing slurry between the different teeth is easy to agglomerate, and leads to a poor preparation effect. Therefore, a flexible fiber tool is introduced, and the elastic force of the flexible fiber is used to destroy the polishing slurry group between the tooth gaps to ensure the smooth flow of the polishing slurry. The flow characteristics of the mechano-rheological polishing slurry ensure that the "flexible fixed abrasive tool" formed by it can maintain a good fit with curved surfaces of different curvatures, so high-quality preparation of the cutting edges of steel drills with different shapes can be achieved.

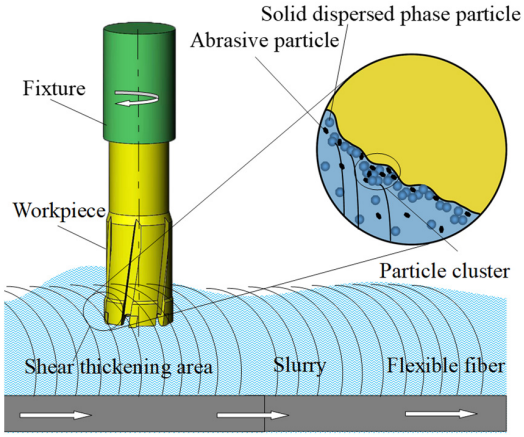

Figure 1. Schematic diagram of FF-FRP treatment of core drill.

3. FF-FRP Experiment for Cutting Edge Preparation of Core Drill

Experimental Setup and Experimental Conditions

Figure 2 shows the schematic diagram (a) and photo (b) of the FF-FRP experimental system for core drill cutting edge preparation. The core drill is immersed in the polishing slurry and rotated clockwise at the speed of 10 r/min, and the polishing tank rotates counterclockwise at a set speed. The distance between the outer edge of the core drill and the wall surface of the polishing tank is 10 mm, and the distance from the cutting edge to the polishing solution surface is recorded as *L*.

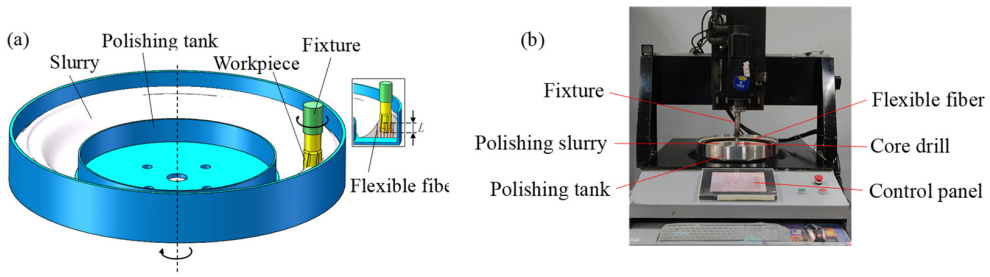

Figure 2. FF-FRP experimental system: (**a**) schematic illustration, (**b**) a photo of the experiment device.

The polishing slurry is a suspension liquid composed of micron-sized polyhydroxy polymer particles (PHHP) mixed with deionized water and abrasive particles. The polishing slurry can produce a shear-thickening effect at a low relative motion speed, and raw materials are easy to obtain, green and pollution-free. Due to the high hardness and high wear resistance of cemented carbide inserts, 8000# diamond powders with an average particle size 1.3 μm were used as abrasive particles in this study. Figure 3 shows the rheological curves of the polishing slurry with different abrasive concentrations. As the concentration increases, the initial viscosity increases and the peak viscosity decreases.

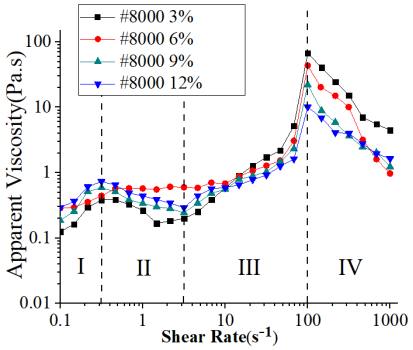

Figure 3. Rheological curves of polishing slurry with different diamond abrasive concentrations.

The experimental object is a cemented carbide core drill with an outer diameter of D = 20 mm. Table 1 shows the mechanical properties of the cemented carbide insert. The experiment mainly studies the effects of polishing speed, abrasive concentration and contact length between flexible fiber and core drill on the core drill edge. A single-factor experimental scheme [26–28] is adopted to design the experiment. The experimental conditions are shown in Table 2. Group 1, group 2 and group 3, respectively, explored the effects of polishing speed, abrasive concentration, contact length on cutting edge radius and surface morphology of the core drill edge. The flexible fiber tool used in the experiment is made of pig bristles with a fiber diameter of 200–250 μm, a fiber height of 30 mm, and a fiber density of 200–250 pieces/cm^2. The flexible fiber tool used in the experiment is made of pig bristles with a fiber diameter of 200–250 μm, a fiber height of 30 mm, and a fiber density of 200–250 pieces/cm^2. The treatment time per trial was 8 min, and the larger variation of the cutting edge radius after treatment means higher preparation efficiency. There are three types of the cutting edges, labelled A_1, A_2, A_3 (as shown in Figure 4), and the two sets of diagonally arranged cutting edges are the same cutting edges. Therefore, three different types of cutting edges are selected as measuring edges, each edge is measured three times, and the average value is taken as the final result.

Table 1. Mechanical property of cemented carbide insert [17].

Material	Density (g/cm^3)	Flexural Strength (MPa)	Hardness (HRA)	Fracture Toughness (MPa m$^{1/2}$)
YG8	14.7	1500	89	2.5

Table 2. Experimental conditions.

Parameters	Values		
	Group 1	Group 2	Group 3
Polishing speed (r/min)	50, 60, 70, 80, 90	80	80
Abrasive concentration (wt.%)	6	3, 6, 9, 12	6
Contact length	7	7	1, 3, 5, 7, 9
Abrasive		Diamond, 8000#	
Processing time per trial (min)		8	

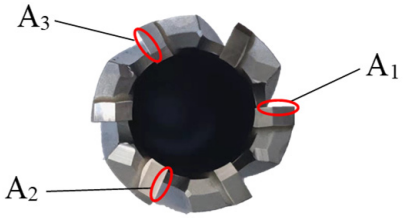

Figure 4. Measuring positions of prepared edges.

The cutting edge radius of the core drill is measured by the Zoller-pom SkpGo blade edge measuring instrument. The measurement method is shown in Figure 5. A total of 100 sections were measured at the cutting edge, and the average of the cutting edge radius of one hundred sections is taken as the final measurement. The roughness of the flank face was measured by Talysurfi-Series (Taylor Hobson), with a trace length 2 mm; the measurements were repeated three times at each measuring point, and the average value of the data was taken as the final result. The surface morphology of the cutting edge was observed with a super-depth-of-field microscope (VHX-100). The initial cutting edge radius of the core drill is 6 ± 2 μm, and the initial flank face roughness of the cutting edge is 107.4 ± 10 nm.

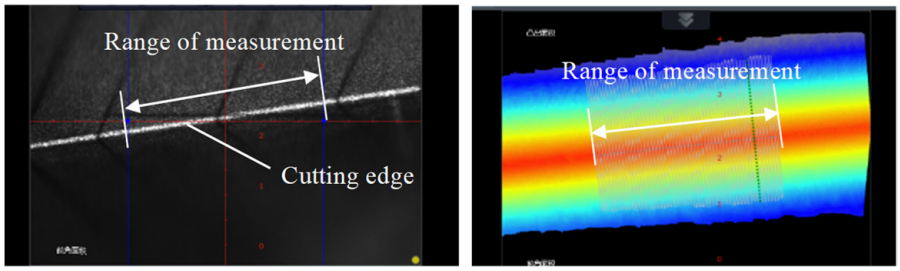

Figure 5. Measuring method of prepared edge radius.

4. Experimental Results and Discussion

4.1. Influence of Polishing Speed

The polishing speed not only affects the hydrodynamics of the polishing slurry, but also determines the force applied by the polishing slurry on the workpiece and abrasive particles [29]. As shown in Figure 6, with the increase of polishing speed, the cutting edge radius of the three groups of A_1, A_2, and A_3 showed a trend of increasing first and then decreasing, and the preparation efficiency first increased and then decreased. When the polishing speed was 80 r/min, the preparation efficiency is the highest. At a low polishing speed, the shear rate of the polishing slurry is low, the strength of shear-thickening effect is weak, the force of the abrasive particles on the workpiece is small, and the preparation efficiency is low. When the polishing speed is too fast, the polishing slurry is thrown to the wall of the polishing tank [30], the mass fraction of abrasive particles involved in cutting edge preparation polishing decreases, and the preparation efficiency decreases. In the preparing process, the angle between the A_2 edge and the bottom of the polishing tank is larger, the flexible fibers exert less force on the A_2 cutting edge, so the preparation efficiency is smaller than A_1 and A_3. As shown in Figure 7, the shape of the A_1 edge is relatively sharp before treatment, with burrs and edge chipping, and the rake and flank face are rough and dull. With the increase of polishing speed, the radius of the cutting edge is significantly increased, the cutting edge is gradually rounded, smooth and has no burrs and other microscopic defects, and the rake and flank face are smooth and close to the mirror effect. The flank face roughness of the cutting edges decreases from 107.4 ± 10 nm to 7.5 ± 2 nm.

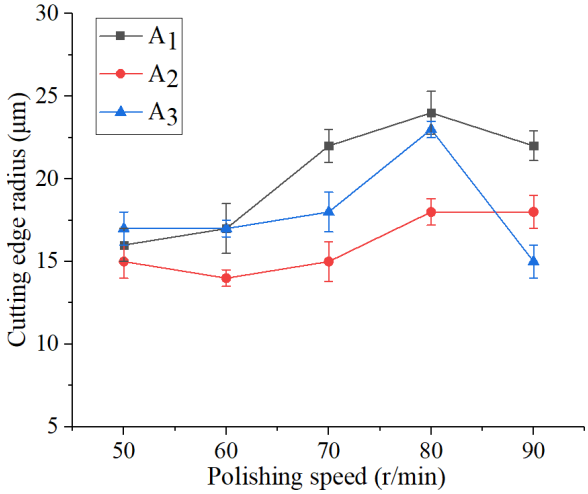

Figure 6. Effect of polishing speed on cutting edge radius.

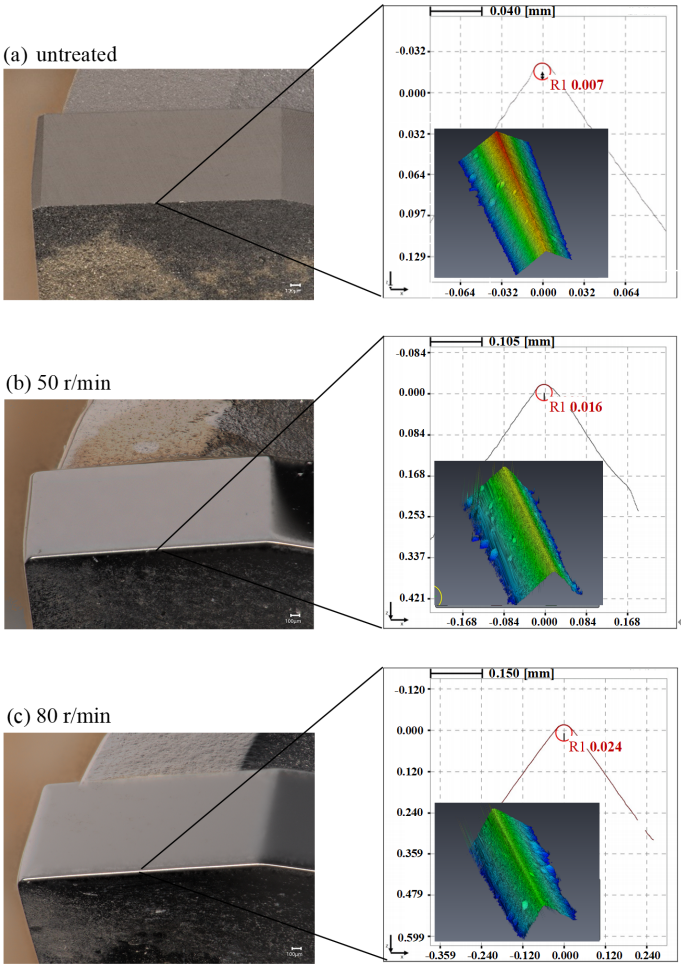

Figure 7. Morphology changes of edge A_1 in cutting edge preparation at different polishing speeds.

4.2. Influence of Abrasive Concentration

As shown in Figure 8, with the increase of abrasive concentration, the cutting edge radius of A_1 and A_3 increased first and then decreased, and the cutting edge radius of A_2 first increased, then decreased, then increased, then decreased. When the abrasive concentration is 12 wt.%, the preparation efficiency is the highest, and the preparation efficiency of A_2 cutting edge is lower than that of A_1 and A_3. The higher the abrasive concentration, the more abrasive particles participating in the removal of the surface material of the workpiece, the material removal efficiency is improved, and the cutting edge radius is further increased. However, excessively high abrasive concentration will cause the deterioration of shear-thickening effect of the polishing slurry [30]. So, the change of the edge at the abrasive concentration of 15 wt.% is not discussed in this article. When the abrasive concentration is 6 wt.% and 9 wt.%, the cutting edge radius does not change much. At this time, the influence of the number of abrasive particles participating in the removal of the preparation effect is related to the influence of the change of the shear-thickening effect of the polishing slurry due to the change of the abrasive concentration on the preparation effect. The preparation efficiency of the A_2 edge is lower than that of A_1 and A_3. The reason is related to the shape and position of the A_2 edge itself. It has been explained in the influence of polishing speed on the edge. As shown in Figure 9, the shape of the A_2 cutting edge is relatively sharp before preparation, with gaps and burrs, and the rake and flank faces are rough and dull, after 8 min of treatment cutting edge preparation with the 3 wt.% abrasive concentration, the cutting edge becomes smooth, the rake and flank faces are also smooth. When the abrasive concentration increases to 9 wt.%, the cutting edge radius increases significantly, the cutting edge was rounded, the burrs and chipping are

not observed on the cutting edge, the transition between the outer edge and the middle edge is natural, and the boundary line is round curved, the rake and flank face are smooth. The flank face roughness of the cutting edges decreases from 110.2 ± 8 nm to 7.5 ± 1 nm.

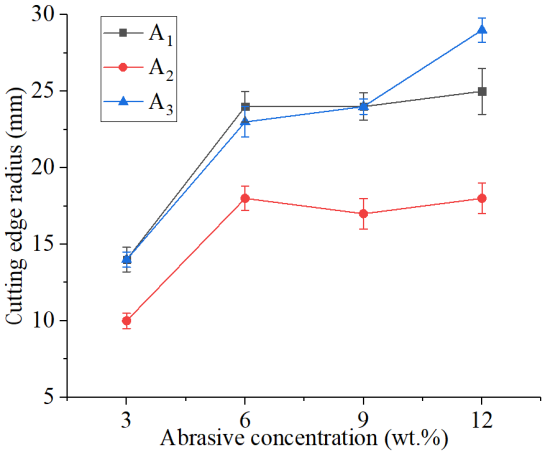

Figure 8. Effect of abrasive concentration on preparation edge radius.

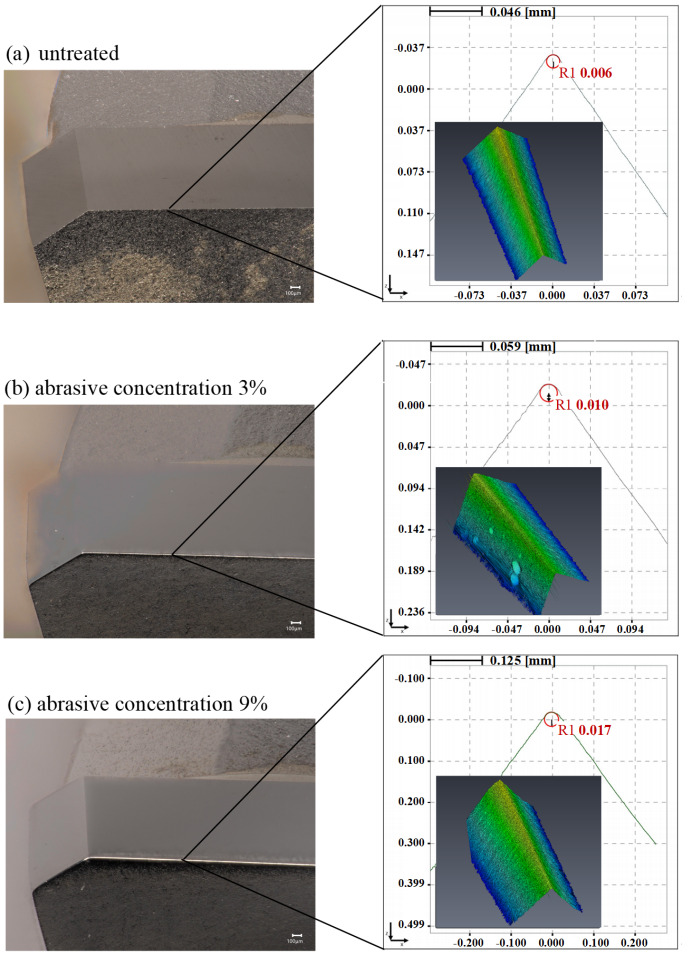

Figure 9. Morphology change of edge A_2 in preparation at different abrasive concentration.

4.3. Influence of the Contact Length between Flexible Fiber and Core Drill

As shown in Figure 10, when the contact length between flexible fiber and core drill increases, the cutting edge radius of the three groups of A_1, A_2, and A_3 increases first and then decreases, and the preparation efficiency first increases and then decreases. The highest preparation efficiency was obtained when the contact length was 7 mm. If contact

length too small, it is difficult for the flexible fibers to break thickened blocks, the polishing slurry cannot flow through the cutting edge well, the material removal rate is reduced, and the preparation efficiency is reduced. As the contact length between flexible fiber and core drill becomes longer, the elastic force of flexible fibers applied to the polishing slurry increases (the relationship between elastic force and flexible fiber length l is $1/l^3$ [31]; that means the shorter the fiber, the greater the elastic force), the preparation efficiency is improved. However, when the contact length is too large, the content of polishing slurry between the flexible fibers becomes less and the removal effect decreases; this is mainly related to the divergence of fibers from bottom to top; in other words, with the increase of contact length, the actual fiber density at the contact position increases and the amount of polishing slurry that can be accommodated between the flexible fibers decreases. When the contact lengths between flexible fiber and core drill are 7 mm and 9 mm, the preparation efficiency of the A_2 cutting edge is not much different from that when the contact length is 5 mm. When the contact length is 7 mm, the preparation efficiency of A_2 is significantly lower than that of A_1 and A_3; at this length, the pressure of the flexible fiber on the cutting edge plays an important role in the material removal rate. The effects of polishing speed and abrasive concentration on the cutting edge were all carried out at a depth of 7 mm, it also confirmed that the preparation efficiency of A_2 was lower than that of A_1 and A_2 because of its own shape and position relationship. As shown in Figure 11, the shape of the A_3 cutting edge is relatively sharp before treatment, and the rake and flank faces are rough and dull. After preparing for 8 min with 3mm contact length, the cutting edge was rounded, the burrs and chipping are not observed on the cutting edge, and the cutting edge radius increases significantly. When the depth continues to increase to 9 mm, the shape of the cutting edge is smooth, the arc of the boundary line of the three-edged rake face becomes larger, and the overall appearance of the rake face is rounded. The flank face roughness of the cutting edges decreases from 106.6 ± 7 nm to 7.1 ± 2 nm.

This paper mainly explores the influence of different factors on preparation efficiency and effect and improves the tool performance by FF-STP method. Reference [32] has put forward an unconventional tool with selective exchange of worn cutting edge, which can improve the surface quality and dimensional accuracy of machine parts, especially improve tool life. It is good for novel tool designs. In addition, reference [33] studied edge inclination angle effect on minimum uncut chip thickness in oblique cutting of C45 steel, which introduces a new area for research on improving the surface quality based on lowering the effect of MUCT on surface roughness. It also puts forward a new idea for improving tool performance.

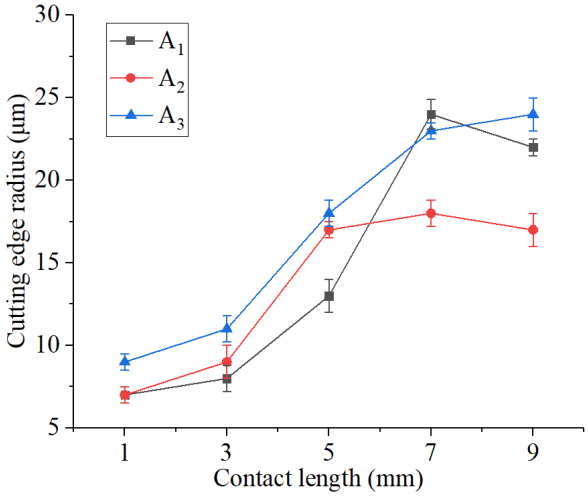

Figure 10. Effect of depth of polishing slurry inserted into core drill on cutting edge radius.

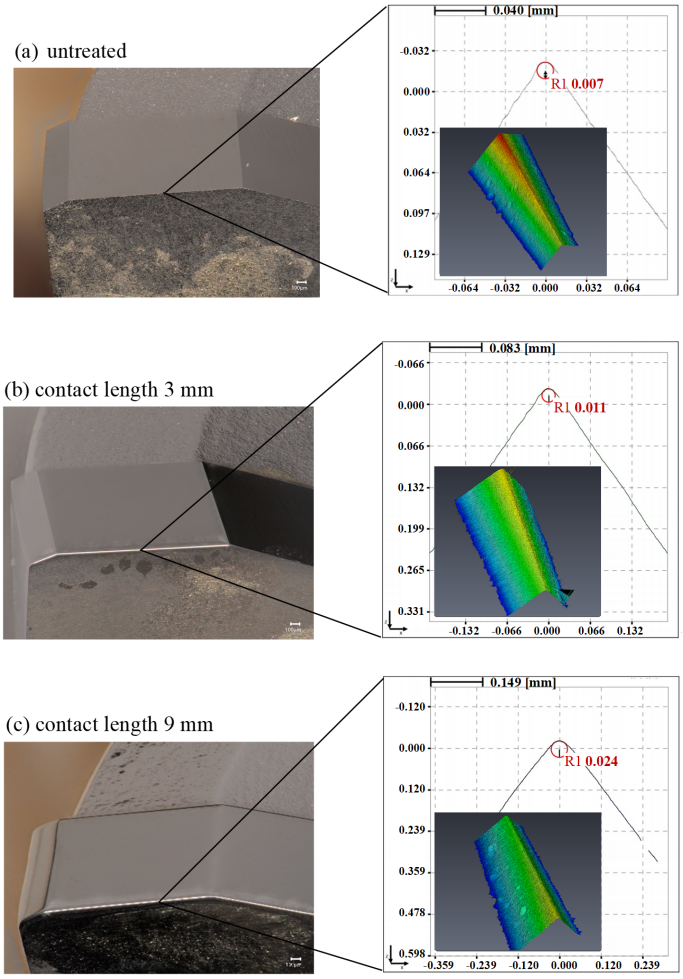

Figure 11. Morphology changes of edge A_3 in cutting edge preparation at different immersion depths.

5. Drilling Tests

Drilling experiments were carried out using the three core drills as presented in Figure 12 with cutting edge radius of 5 μm (without treatment), 14 μm (with 4 min of treatment) and 27 μm (with 6 min of treatment) under polishing conditions of 80 r/min polishing speed, 6 wt.% abrasive concentration and 7 mm contact length. The cutting edge radius measurement result in shown in Figure 13. The experimental conditions are shown in Table 3, the constant cutting rate and the feed rate was set at 600 r/min and 25 mm/min. Figure 14 presents the drilling process; no coolant is allowed during drilling. The workpiece is shown in Figure 15, and the material is Q235 steel (ASTM A36) [34]. Each core drill is continuously processed with nine holes in the steel plate. The performance of the core drill was also assessed by the measurement of the drilled holes' roughness and cutting temperature [35,36]. Cutting heat has many adverse effects in metal cutting process, so it is necessary to take measures to reduce and limit the cutting heat [37]. In addition, high roughness of the hole wall will lead to a degradation in the product quality and reliability of the product [38]. The cutting temperature is measured by thermal imager (FOTRIC 220s, temperature measurement accuracy ±2 °C), the working principle is to use a thermographic or thermal camera to detect the radial heat from cutting tool and workpiece for determination of the temperature [39]. And the roughness of the hole was measured by the Form Talysurf i-Series (Taylor Hobson, Leicester, UK) with a trace length is 2 mm, the roughness of four points around the hole wall was measured uniformly along the circle, and the average value of the four points was taken as the final roughness result.

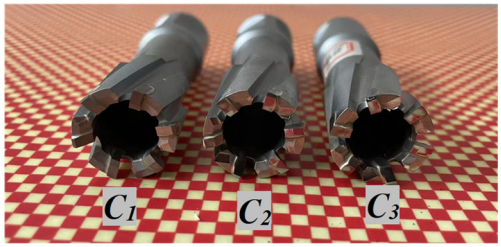

Figure 12. Core drills to be tested. C_1: before treatment, r = 5 µm. C_2: after treatment, r = 14 µm. C_3: after treatment, r = 27 µm.

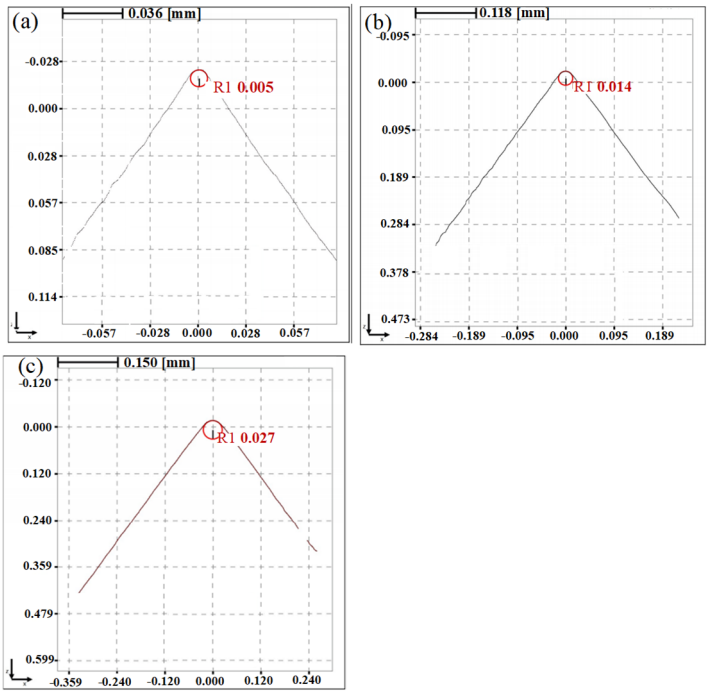

Figure 13. Cutting edge radius measurement result: (**a**) C_1, r = 5 µm (**b**) C_2, r = 14 µm (**c**) C_3, r = 27 µm.

Table 3. The experimental conditions.

Processing Condition	Parameter
Workpiece	Q235 steel (ASTM A36)
Lubrication	dry drilling
Rotation speed of core drill	600 r/min
Feed rate	25 mm/min

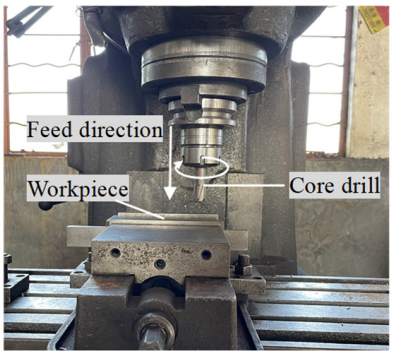

Figure 14. Drilling process.

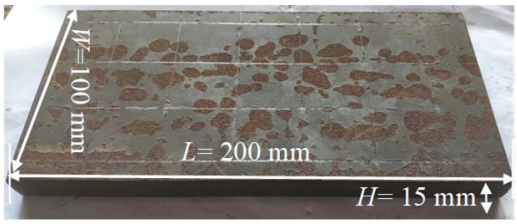

Figure 15. The workpiece: Q235 steel.

Figure 16 shows the workpiece after being drilled. The cutting temperature and roughness of core drill with different cutting edge radius after treatment were compared, the real-time temperature cloud map of C_1, C_2, C_3 core drill during drilling is showed in Figure 17, and the test results are shown in Figures 18 and 19. The cutting temperature generated during machining can be reduced effectively by increasing the radius of the cutting edge. The highest cutting temperature before treatment can reach 148.6 °C. The highest cutting temperature of core drilling with cutting edge radius r = 14 μm and r = 27 μm are 122.4 °C and 124.7 °C, respectively. The cutting heat generated by core drilling after treatment is significantly lower than that without preparation. The average roughness of nine drilled holes with untreated core drill is R_a 700.4 nm, the surface are R_a 510.5 nm and R_a 541.2 nm after treatment with r = 14 μm and r = 27 μm, respectively. The roughness of hole wall can be reduced effectively by increasing the cutting edge radius within a certain range, and when the core drill is processed with r = 14 μm, the roughness of hole wall is the minimum. When the cutting edge radius continues to increase to r = 27 μm, the roughness of hole wall increases again. Heat is generated by the friction between the workpiece and the core drill, core drills with lower roughness produce smoother holes and less cutting heat during drilling. The influence of different cutting edge radius on cutting force and the material removal mechanism will be investigated in the future works.

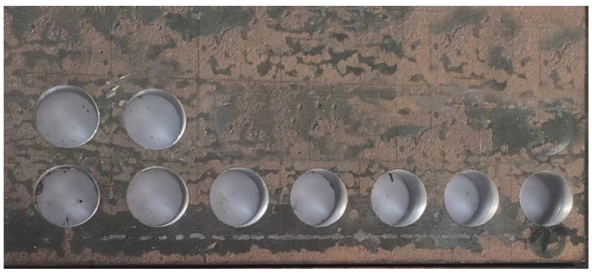

Figure 16. The workpiece after being drilled.

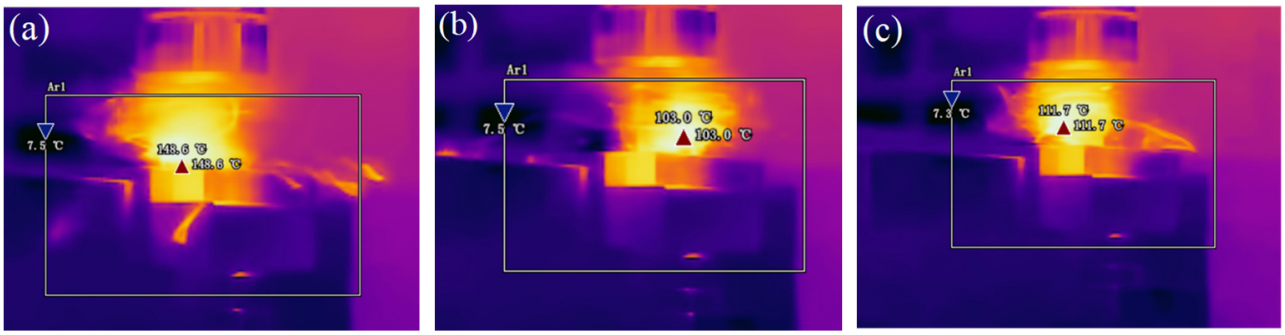

Figure 17. Real-time temperature cloud map of C_1 (**a**), C_2 (**b**), C_3 (**c**) core drill during drilling.

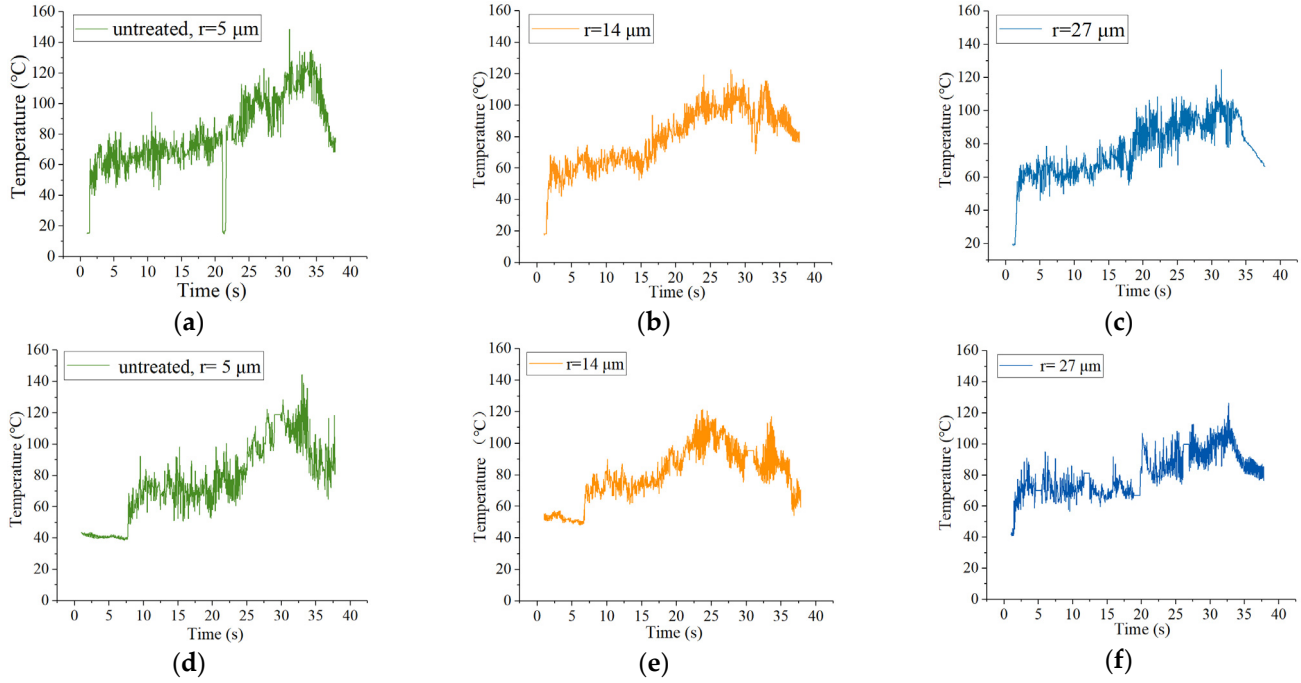

Figure 18. Trend diagram of cutting temperature over time. The first hole drilling: (**a**) before treatment, r = 5 μm. (**b**) after treatment, r = 14 μm. (**c**) after treatment, r = 27 μm. The sixth hole drilling: (**d**) before treatment, r = 5 μm. (**e**) after treatment, r = 14 μm. (**f**) after treatment, r = 27 μm.

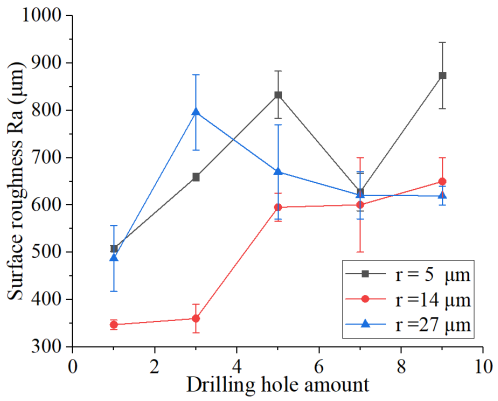

Figure 19. Roughness of the hole wall under different number of holes.

6. Conclusions

The FF-STP was used to prepare the cutting edge of the core drill. The effect of polishing speed, abrasive concentration, and the flexible fiber contact length with the core drill on the cutting edge radius and surface morphology of the core drill edge were studied, and the drilling experiments were carried out on the core drill after treatment. The conclusions are as follows:

(1) Due to the different shapes of cutting edges, the effects of polishing speed, abrasive concentration, and depth of immersion in the flexible fiber of the core drill on the change of the cutting edge radius is different in cutting edge treatment for 8 min. The A_2 edge has lower preparation efficiency than A_1 and A_3 because of its specific shape.

(2) The cutting edge radius increases with the increase of polishing speed, abrasive concentration and contact length, but too large polishing speed and contact length lead to a decline oin the preparation efficiency.

(3) Under the selected processing conditions, the cutting edge radius increases from the initial 5 μm to 14 μm and 27 μm after cutting edge preparation for 4 and 6 min, respectively,

the cutting edge is gradually rounded, smooth and has no burrs and other microscopic defects, and the average roughness of the flank face decreases from 110.4 ± 10 nm to 8.0 ± 3 nm.

(4) The maximum cutting temperature (122.4 °C) in the process with the treated core drill (radius r = 14 μm) is about 20 °C lower than that with untreated one, and the roughness of the drilled hole (R_a 510.5 nm) is about 189.9 nm lower. The drilling quality is obviously improved. However, too large a cutting edge radius (radius r = 27 μm) will cause an increase of the roughness.

(5) The drilling experiments indicates that FF-STP can change the cutting edge, improve the surface quality and performance of the core drill. In the future, the influence of different cutting edge radiuses on the material removal mechanism, cutting force and tool wear will be investigated.

Author Contributions: Conceptualization, L.S., Y.Z., Y.D. and B.L.; methodology, L.S., Y.Z. and B.L; formal analysis, L.S.; investigation, Y.D.; resources, B.L.; writing—original draft preparation, L.S., Y.Z.; writing—review and editing, L.S., B.L.; visualization, L.S., Y.D.; supervision, B.L.; project administration, L.S., B.L.; funding acquisition, B.L. All authors have read and agreed to the published version of the manuscript.

Funding: This research was supported by the financial support from national natural Science Foundation of China (52175441) and Zhejiang Provincial Natural Science Foundation of China (LD22E050010).

Data Availability Statement: Not applicable.

Conflicts of Interest: The authors declare no conflict of interest. The funders had no role in the design of the study; in the collection, analyses, or interpretation of data; in the writing of the manuscript; or in the decision to publish the results.

References

1. Binali, R.; Kuntoğlu, M.; Pimenov, D.Y.; Usca, Ü.A.; Gupta, M.K.; Korkmaz, M.E. Advance monitoring of hole machining operations via intelligent measurement systems: A critical review and future trends. *Measurement* **2022**, *201*, 111757. [CrossRef]
2. Aamir, M.; Giasin, K.; Tolouei-Rad, M.; Vafadar, A. A review: Drilling performance and hole quality of aluminium alloys for aerospace applications. *J. Mater. Res. Technol.* **2022**, *9*, 12484–12500. [CrossRef]
3. Jiao, Y. Development of cemented carbide steel plate drills. *Metal Work. (Metal Cut.)* **2011**, *3*, 41–42.
4. Qi, Z.; Chen, X. Research progress of cemented carbide cutting tools. *Mater. Res. Appl.* **2019**, *13*, 347–354.
5. Wu, B.; Chen, Z.; Huang, L.; Xu, Q.; Xu, H. State of art in cutting tool preparation technologies. *Tool Technol.* **2019**, *53*, 8–14.
6. Li, Z.; Wang, H.; Su, H.; Liu, H. Application of abrasive electrochemical machining in carbide tool edge honing. *J. Dalian Univ. Technol.* **2019**, *38*, 141–145.
7. Biermann, D.; Terwey, I. Cutting edge preparation to improve drilling tools for HPC processes. *CIRP J. Manuf. Sci. Technol.* **2008**, *1*, 76–80. [CrossRef]
8. Zou, Y. *Research on Key Technology of Ultrasonic Vibration Rounding with Flat End Milling Cutter*; Zhejiang University of Technology: Hangzhou, China, 2019.
9. Lv, D.; Wang, Y.; Yu, X.; Chen, H.; Gao, Y. Analysis of abrasives on cutting edge preparation by drag finishing. *Int. J. Adv. Manuf. Technol.* **2022**, *119*, 3583–3594. [CrossRef]
10. Peter, P.; Boris, P.; Tomáš, V.; Jozef, P.; Šimna, V. Cutting edge radius preparation. *Mater. Today Proc.* **2020**, *22*, 212–218. [CrossRef]
11. Denkena, B.; de Leon, L.; Bassett, E.; Rehe, M. Cutting edge preparation by means of abrasive brushing. *Key Eng. Mat.* **2010**, *438*, 1–7. [CrossRef]
12. Kang, Y.; Derouach, H.; Berger, N.; Herrmann, T.; L'Huillier, J. Experimental research of picosecond laser based edge preparation of cutting tools. *J. Laser Appl.* **2020**, *32*, 022043. [CrossRef]
13. Vopát, T.; Podhorský, Š; Sahul, M.; Haršáni, M. Cutting edge preparation of cutting tools using plasma discharges in electrolyte. *J. Manuf. Process.* **2019**, *46*, 234–240. [CrossRef]
14. Yussefian, N.; Koshy, P. Application of foil electrodes for electro-erosion edge honing of complex-shaped carbide inserts. *J. Mater. Process. Technol.* **2013**, *213*, 434–443. [CrossRef]
15. Liu, Y.; Zou, B.; Zhang, S. Study on edge preparation of cemented carbide inserts based on micro-blasting jet technology. *Tool Technol.* **2017**, *51*, 16–20.
16. Li, M.; Lyu, B.; Yuan, J.; Dong, C.; Dai, W. Shear-thickening polishing method. *Int. J. Mach. Tools Manuf.* **2015**, *94*, 88–99. [CrossRef]
17. Lyu, B.; Dong, C.; Yuan, J.; Sun, L.; Li, M.; Dai, W. Experimental study on shear thickening polishing method for curved surface. *Int. J. Nanomanuf.* **2017**, *13*, 81–95. [CrossRef]
18. Li, M.; Huang, Z.; Dong, T.; Tang, C.; Lyu, B.; Yuan, J. Surface quality of zirconia (ZrO2) parts in shear-thickening high-efficiency polishing. *Procedia CIRP* **2018**, *77*, 143–146. [CrossRef]

19. Yang, Y.; Lyu, B.; Song, Z.; Shao, Q.; Ke, M.; Yuan, J.; Nguyen, D. Optimization experiment for chemistry enhanced shear thickening polishing of alμminμm alloy conical mirror. *Surf. Technol.* **2020**, *49*, 329–337.
20. Lyu, B.; He, Q.; Chen, S.; Shao, Q.; Chen, Y.; Geng, Z. Experimental study on shear-thickening polishing of cemented carbide insert with complex shape. *Int. J. Adv. Manuf. Technol.* **2019**, *103*, 585–595. [CrossRef]
21. Shao, Q.; Shao, L.; Lyu, B.; Zhao, P.; Wang, J.; Yuan, J. Parameter optimization by Taguchi method for shear thickening polishing process of quartz glass. *Surf. Technol.* **2021**, *50*, 85–93.
22. Lyu, B.; Ke, M.; Fu, L.; Duan, S.; Shao, Q.; Zhou, Y.; Yuan, J. Experimental study on the brush tool-assisted shear-thickening polishing of cemented carbide insert with complex shape. *Int. J. Adv. Manuf. Technol.* **2021**, *115*, 2491–2504. [CrossRef]
23. Chan, J.; Koshy, P. Tool edge honing using shear jamming abrasive media. *CIRP Ann.* **2020**, *69*, 289–292. [CrossRef]
24. Span, J.; Koshy, P.; Klocke, F.; Muller, S.; Coelho, R. Dynamic jamming in dense suspensions: Surface finishing and edge honing applications. *CIRP Ann. Manuf. Technol.* **2017**, *66*, 321–324. [CrossRef]
25. Shao, L.; Zhou, Y.; Fang, W.; Wang, J.; Wang, X.; Deng, Q.; Lyu, B. Preparation of cemented carbide insert cutting edge by flexible fiber-assisted shear thickening polishing method. *Micromachines* **2022**, *13*, 1631. [CrossRef]
26. Zhang, R.; Chen, X.; Gong, F.; Li, L. Research on the influence factors of high speed spindle's bearing temperature. *Mach. Tools Hydraul.* **2020**, *48*, 27–30.
27. Chang, S.; Sun, X.; Ma, L.; Yang, Z.; Wang, F. Research on the preparation and properties of a hard anodized oxide film based on the single factor experiment. *Chem. Adhes.* **2020**, *42*, 330–333.
28. Xiao, G.; Huang, Y. Research and analysis the titanium alloy belt grinding belt life expectancy based on the single factor experiment. *Mech. Des. Manuf.* **2010**, *234*, 175–177.
29. Galindo-Rosales, F.J.; Rubio-Hernández, F.J.; Sevilla, A.; Ewoldt, R.H. How Dr. Malcom M. Cross may have tackled the development of "An apparent viscosity function for shear thickening fluids". *J. Non-Newt. Fluid Mech.* **2011**, *166*, 1421–1424. [CrossRef]
30. Lyu, B.; Shao, Q.; Hang, W.; Chen, S.; He, Q.; Yuan, J. Shear thickening polishing of black Lithium Tantalite Substrate. *Int. J. Precis. Eng. Manuf.* **2020**, *21*, 1663–1675. [CrossRef]
31. Dimov, Y.V.; Podashev, D.B. Edge forces in machining by abrasive brushes. *Rus. Eng. Res.* **2017**, *37*, 117–121. [CrossRef]
32. Mikolajczyk, T.; Paczkowski, T.; Kuntoglu, M.; Patange, A.; Binali, R. Research on using an unconventional tool for increasing tool life by selective exchange of worn cutting edge. *Appl. Sci.* **2022**, *13*, 460. [CrossRef]
33. Mikołajczyk, T.; Latos, H.; Szczepaniak, Z.; Paczkowski, T.; Pimenov, D.; Giasin, K.; Kuntoğlu, M. Theoretical and experimental research of edge inclination angle effect on minimum uncut chip thickness in oblique cutting of C45 steel. *Int. J. Adv. Manuf. Technol.* **2022**, *124*, 2299–2312. [CrossRef]
34. Ke, R. Carbon structural steel and its application. *Metal World* **1997**, *4*, 6–7.
35. Yellowley, I.; Barrow, G. The influence of thermal cycling on tool life in peripheral milling. *Int. J. Mach. Tool Des. Res.* **1976**, *16*, 1–12. [CrossRef]
36. Bhatia, S.M.; Pandey, P.C.; Shan, H.S. Failure of cemented carbide tools in intermittent cutting. *Precis. Eng.* **1979**, *1*, 148–152. [CrossRef]
37. Song, A.; Yue, X.; Liu, J.; Zhai, Y.; Wang, P.; Zhang, P.; Yu, X. Research on influence mechanism of cutting performance of 7075-T6 aluminum alloy. *Tool Eng.* **2022**, *56*, 37–43.
38. Liu, Y.; Zhang, H.; Fu, L.; Wang, L. Study on tool wear and hole wall quality of drilling PCB with concave edge twist drills. *Print. Circ. Inf.* **2014**, *31*, 39–51.
39. Kuntoğlu, M.; Salur, E.; Gupta, M.; Sarıkaya, M.; Pimenov, D. A state-of-the-art review on sensors and signal processing systems in mechanical machining processes. *Int. J. Adv. Manuf. Technol.* **2021**, *116*, 2711–2735. [CrossRef]